



Published in final edited form as:

Nat Med. 2007 July ; 13(7): 828–835.

Altered recognition of antigen is a novel mechanism of CD8⁺ T cell tolerance in cancer

Srinivas Nagaraj¹, Kapil Gupta², Vladimir Pisarev³, Leo Kinarsky³, Simon Sherman³, Loveleen Kang¹, Donna Herber¹, Jonathan Schneck², and Dmitry I. Gabrilovich¹

¹ H. Lee Moffitt Cancer Center, University of South Florida, 12902 Magnolia Dr. Tampa, FL, 33647

² John Hopkins University Medical School, 720 Rutland Ave., Baltimore, MD, 21205

³ University of Nebraska Medical Center and Eppley Cancer Center, 986805 Nebraska Medical Center, Omaha NE 68198

Abstract

Antigen-specific CD8⁺ T-cell tolerance is one of the major mechanisms of tumor escape. Recent studies have shown that this tolerance was induced by myeloid-derived suppressor cells (MDSC). Using *in vivo* models we have found that MDSC directly disrupted the binding of the specific peptide-MHC (pMHC) dimers to CD8⁺ T cells via nitration of tyrosines within TCR/CD8 complex, which resulted in the inability of CD8⁺ T cells to bind pMHC and respond to the specific peptide. These cells retained their ability to respond to non-specific stimulation. Nitration of TCR/CD8 was induced by MDSC via hyperproduction of reactive oxygen species (ROS) and peroxynitrite during direct cell-cell contact. Molecular modeling suggested specific sites of nitration that could affect conformational flexibility of TCR/CD8 and its interaction with pMHC. This data demonstrates novel mechanisms of T-cell tolerance in cancer that also can be pertinent to many pathological conditions associated with accumulation of MDSC.

Introduction

T-cell tolerance play an important role in tumor escape¹. It is also one of the major obstacles limiting the effect of cancer vaccines. Previous studies have established that antigen presenting cells (APC) are primarily responsible for the induction of tumor-induced T-cell tolerance^{2,3}. We and others have recently identified a group of Gr-1⁺CD11b⁺ MDSC that are primarily responsible for tumor-associated CD8⁺ T-cell tolerance^{4,5}. These are immature cells comprised of precursors of macrophages, granulocytes, DCs, and myeloid cells at earlier stages of differentiation, and display the ability to suppress immune response *in vitro* via direct cell-cell contact (rev. in ⁶⁻⁹). Accumulation of similar cells was described in cancer patients¹⁰⁻¹². MDSC induce antigen-specific MHC class I restricted tolerance of CD8⁺ T cells *in vivo*⁴. This phenomenon may provide the mechanism of antigen-specific inhibition of immune response in cancer and may explain the difficulties in maintaining the antigen-specific immune response after vaccination in cancer patients. However, the mechanism of MDSC-induced CD8⁺ T-cell tolerance remained unclear.

We asked what mechanism of CD8⁺ T-cell tolerance is employed by MDSC. There are two basic mechanisms of T-cell tolerance: deletion and anergy. Existing data *in vitro* and *in vivo* indicate that MDSC do not induce T-cell death and the deletion of antigen-specific T cells⁴⁻⁹. Although much is known about the biochemical basis of T-cell anergy, the antigen-

specific nature of T-cell tolerance remains less understood^{13,14}. Using an experimental model *in vivo* we demonstrated that MDSC, via generation of ROS and peroxynitrite, induced modification of TCR and CD8 molecules that resulted in the loss of ability of CD8⁺ T cells to bind pMHC and induction of antigen-specific non-responsiveness of peripheral CD8⁺ T cells. This represents a new mechanism of T-cells tolerance in cancer and may be applicable to a number of pathological conditions (e.g. infection, inflammation, trauma) associated with the accumulation of MDSC overproducing peroxynitrite.

Results

MDSC disrupt pMHC binding to CD8⁺ T cells

We used an experimental model where the direct effect of MDSC on antigen-specific CD8⁺ T cells could be evaluated *in vivo* (Fig. S1). In this model, OT-1 T cells (CD45.1⁻) were transferred to naïve CD45.1⁺ congenic recipients. MDSC from EL-4 tumor-bearing mice were transferred two days later and mice were immunized with specific peptide. LN cells were collected 10 days after immunization. By that time all transferred MDSC either differentiated into mature myeloid cells or died (15 and data not shown) and did not directly interfere with any assay performed in LN. Donor's CD45.1⁻CD8⁺ T cells from mice that received MDSC had substantially reduced ability to bind specific pMHC-Ig dimers than cells from control mice (Fig. 1a, b). Similar effect was observed in a different experimental system where T cells from 2C transgenic mice were adoptively transferred to naïve congenic mice and 2C specific peptide was used for immunization (Fig. S2a). Repeated experiments demonstrated that MDSC administration did not affect the expression of TCR or CD8 molecules on the surface of T cells (Figs. 1c and S2).

LN cells isolated from mice treated with MDSC were re-stimulated *in vitro* with escalating concentrations of the specific peptides. The number of IFN- γ producing CD8⁺ T cells was evaluated in ELISPOT assay. CD8⁺ T cells from MDSC-treated mice did not respond to the specific peptide. It was not improved even by a 50-fold increase in the peptide concentration (Fig. 1d). This data was confirmed in CTL assay against EL-4 and T2-K^b target cells. In both experimental models (OT-1 and 2C) T cells from control immunized mice demonstrated peptide-specific CTL activity against target cells. In contrast, T cells from mice treated with MDSC did not recognize specific targets. Increased peptide concentration used to load target cells did not result in an improved CTL killing (Figs. 1e and S2c).

To address the possible role of TCR affinity in MDSC-mediated CD8⁺ T-cell tolerance we used three peptides with different affinity to 2C TCR. SIYRYYYGL (SIY) has high affinity, EQYKFYSV (dEV8) has intermediate affinity, and LSPFPFDL (p2Ca) has low affinity^{16, 17}. SIY peptide induced potent response of 2C CD8⁺ T cells and transfer of MDSC completely abolished this response (Fig. 1f). CD8⁺ T-cell response to DEV8 peptide was much weaker. It also was blocked by MDSC. No response was detected against p2Ca peptide.

The mechanism of MDSC-induced disruption of pMHC binding to CD8⁺ T cells

Previous studies have shown that MDSC produce high level of ROS⁸. To clarify the role of ROS in MDSC-induced T-cell tolerance *in vivo* we used mice lacking a critical component of NADPH complex gp91^{phox}¹⁸. MDSC from gp91^{phox}^{-/-} mice have little or no ROS but maintain the level of MHC class I expression (data not shown). In contrast to MDSC from wild-type tumor-bearing mice, MDSC isolated from gp91^{phox}^{-/-} tumor-bearing mice were not able to induce CD8⁺ T-cell tolerance (Fig. 2a). O₂⁻ after interaction with NO forms peroxynitrite (ONOO⁻) with a high biological activity¹⁹. MDSC produce a high level of peroxynitrite²⁰. To evaluate the possible role of ONOO⁻ in MDSC-mediated T-cell tolerance, mice after adoptive transfer of OT-1 T cells and MDSC, were treated with uric acid (UA), a

compound that specifically neutralizes peroxynitrite^{21,22}. UA completely abrogated tolerogenic effect of MDSC (Fig. 2b). Previous study has described the ability of UA in crystal form to activate APC²³. We used a soluble form of UA. To directly evaluate its possible effect on APC activation, mice were treated for 48 h with UA and phenotype and function of DCs were evaluated. No differences between control and treated mice were found (data not shown). In contrast to activated macrophages, MDSC often don't have significant up-regulation of NO^{20,24}. To elucidate the role of NO in MDSC mediated T-cell tolerance we used iNOS deficient mice. These mice cannot up-regulate NO production in response to different stimuli. However, they retain a basal level of NO production because of activity of other NOS, primarily eNOS²⁵. MDSC from iNOS^{-/-} tumor-bearing mice had the same ability to induce CD8⁺T-cell tolerance as MDSC from wild-type tumor-bearing mice (Fig. 2c). This data indicates that up-regulation of ROS but not NO was primarily responsible for MDSC-mediated CD8⁺T-cell tolerance. Neutralization of peroxynitrite with urea completely abrogated MDSC-mediated decrease in the binding of the specific pMHC to CD8⁺T cells *in vitro* (Fig. 2d) suggesting critical role of peroxynitrite in the disruption of pMHC binding to CD8⁺T cells.

To verify possible role of ONOO⁻ in CD8⁺T cell tolerance we used a donor of peroxynitrite, 3-morpholiniosydnonimine (SIN-1). OT-1 T cells were pre-treated for 30 min with different concentration of SIN-1 and then stimulated with peptide-pulsed DCs or with PHA. SIN-1 at concentration 1 mM did not affect cell viability (data not shown) but completely abrogated peptide-specific CD8⁺T-cell proliferation and IFN- γ production (Fig. 3 a-b) and substantially reduced specific pMHC binding to CD8⁺T cells (Fig. 3c) while not affecting the expression of TCR or CD8 on T cell surface (Fig. 3d). PHA-inducible T-cell proliferation was not affected (Fig. 3a), whereas IFN- γ production was reduced but still remained substantially higher than in control (Fig. 3b). An increased dose of SIN-1 resulted in progressive decrease in cell viability (data not shown), T-cell proliferation and complete abrogation of IFN- γ production (Fig. 3a-b). This data demonstrates that at a relatively low dose SIN-1 reduces the pMHC binding and blocks peptide-specific responses, while having a limited effect on non-specific stimulation of CD8⁺T cells. This was similar to the effect exerted by MDSC *in vivo*.

The role of MDSC induced nitration of TCR complex in CD8⁺T-cell tolerance

The main effect of ONOO⁻ is its ability to modify proteins via oxidation or nitration of different aminoacids. One of the major targets of ONOO⁻ activity is a tyrosine, which creates nitrotyrosine (NT). Nitration of Tyr is relatively stable²⁶ and has been shown to impede the function of the proteins through alteration of the hydrogen-bond, van der Waals, and electrostatic network²⁷. We hypothesized that nitration of Tyr within the pMHC-TCR complex might increase its rigidity and disable its integrity. Molecular modeling of 2C TCR demonstrated that nitration of tyrosine in several sites of TCR and CD8 molecules would dramatically alter recognition of pMHC (Figs. S3 and S4).

We asked whether MDSC could actually cause nitration of TCR-CD8 in antigen-specific CD8⁺T-cells. LN cells were isolated from mice after adoptive transfer of OT-1 T cells, MDSC, and immunization. Donor's peptide-specific CD8⁺V α ₂⁺T cells and recipient's CD8⁺V α ₂⁻T cells were gated and the level of NT on cell surface was evaluated using NT-specific antibody (Fig. 4a). CD8⁺V α ₂⁺ and CD8⁺V α ₂⁻ cells from control immunized mice showed similar levels of NT expression. In contrast, CD8⁺V α ₂⁺ cells from MDSC recipients had a much higher level of NT (Fig. 4a). OT-1 CD8⁺T cells were pre-activated with specific peptide for 72 h and then incubated for 48 h with MDSC isolated from tumor-bearing mice. MDSC substantially increased the level of NT in OT-1 CD8⁺ cells (Fig. 4 b,c). MDSC isolated from gp91^{phox-/-} but not from iNOS^{-/-} mice had failed to induce NT expression on T-cell surface (Fig. 4b). Treatment of MDSC with ROS inhibitor sodium dismutase (SOD) as well as NO synthase inhibitor L-NMMA blocked MDSC inducible increase in NT level (Fig. 4c). L-NMMA inhibits

activity of eNOS as well as iNOS and thus reduces basal level of NO production²⁸, which may explain the difference from the results with iNOS^{-/-} MDSC.

Next, we incubated for 48 h activated OT-1 T cells with MDSC in the presence of specific peptide. T cells were isolated and whole cell lysates were analyzed using Western blotting and NT-specific antibody. Treatment of T cells with MDSC resulted in appearance of several bands positive for NT (Fig. 4d). Treatment of the membranes with sodium dithionite, which causes chemical reduction of nitrotyrosine to aminotyrosine, completely eliminated binding (Fig. 4d) indicating that detected bands indeed contained NT. We asked whether TCR and CD8 molecules could be the targets for MDSC-mediated nitration. Proteins were precipitated with antibodies against TCR β , CD8, or control IgG, subjected to electrophoresis and then probed with NT-specific antibody. MDSC induced a substantial increase in the level of NT in both TCR β and CD8 (Fig. 4e).

Interaction between MDSC and CD8⁺ OT-1 T cells in the presence of specific peptide was evaluated using confocal microscopy. Practically all Gr-1⁺ MDSC were positive for NT localized both on the membrane and in cytoplasm (Fig. 5a). CD8⁺ T cells were NT negative. After 5 h of incubation direct contacts between Gr-1⁺ MDSC and CD8⁺ OT-1 T cells were readily detectable (Fig. 5b). NT in CD8⁺ T cells was primarily localized at the membrane at point of interaction between MDSC and CD8⁺ T cells (Fig. 5c). After 48 h incubation with MDSC diffuse membrane NT staining of CD8⁺ T cells was evident (Fig. 5d). We asked whether NT-positive CD8⁺ T cells could be found in LN from tumor-bearing hosts. We studied LN obtained from 6 individuals with breast and head and neck cancer. Only LNs free of tumor cells were evaluated. As a control lymphoid tissues (tonsils) from two tumor-free persons were used. Very few NT⁺CD8⁺ T cells were found in control samples. In contrast, LN from cancer subjects contained detectable NT⁺CD8⁺ T cells (Figs. S5 and 5e).

Reversal of MDSC-induced CD8⁺ T-cell tolerance

MDSC-induced CD8⁺ T-cell tolerance persisted for at least 3 weeks. The level of response in control mice gradually decreased with time (Fig. S6 a-b). However, 22 days after immunization peptide-specific response was still detectable in LN of control, but not of MDSC-treated mice (Fig. S6b). Stimulation with peptide-loaded LPS activated mDCs but not iDCs overcome MDSC-induced T-cell tolerance (Fig. 6a). Next, we asked if CD8⁺ T-cell tolerance could be observed in tumor-bearing mice. These mice would have “natural” tumor-associated antigens and MDSC. We provided only the source of antigen-specific T-cells. Two tumors were used: EL-4 cells expressing ovalbumin (EG-7) and parental EL-4 tumor. Our previous studies have determined that both EL-4 and EG-7 tumor resulted in an accumulation of MDSC, which could process and present OVA-derived epitope on their surface⁴. OT-1 T-cells were transferred to EL-4 and EG-7 tumor-bearing mice. Mice were sacrificed 7 days later. LNs from control mice contained very few Gr-1⁺ cells, whereas LNs from tumor-bearing mice were packed with these cells (Fig. S7 a-b) located in T-cell areas in direct contact with CD8⁺ T cells (Fig. S7c). LN cells were stimulated with specific or control peptides and the responses were evaluated in IFN- γ ELISPOT assay. Control tumor-free mice demonstrated low (since T cells were not activated *in vivo*) but clearly detectable specific response. A similar response was found in EL-4 tumor-bearing mice. In sharp contrast, no specific response was observed in LN from EG-7 tumor-bearing mice (Fig. 6b). The levels of NT in recipient's V α 2⁻CD8⁺ T cells were similar in all groups of mice. However, it was significantly higher in donor's V α 2⁺CD8⁺ T cells from EG-7 tumor-bearing mice than from control or EL-4 tumor-bearing mice (Fig. 6c).

To identify potential role of peroxynitrite in this process EG-7 tumor-bearing mice were treated with daily i.p. injections of UA starting from the day of adoptive transfer of OT-1 T cells. Seven days later LN cells were isolated and re-stimulated with control or specific peptides. In tumor-bearing mice OT-1 CD8⁺ T cells lost the ability to respond to stimulation with specific peptide

as was documented in IFN- γ ELISPOT (Fig. 6d) or CTL assays (Fig. 6e). Treatment with UA completely prevented the development of T-cell tolerance (Fig. 6d,e). To evaluate a possibility that UA can induce non-specific T-cell activation naïve C57BL/6 mice were treated with daily UA i.p. injections for 7 days. Spleen and LN T cells were analyzed for the expression of CD25 and CD69 molecules and for proliferation in response to different stimuli. Treatment with UA did not result in activation of T cells (Fig. S8).

Next we addressed a possibility that block of peroxynitrite may improve antitumor effect of cancer vaccine in non-transgenic experimental system. MC38 tumor was established in C57BL/6 mice. On day 10 after tumor inoculation mice were split into four groups with equal tumor size. Mice in treatment group were immunized with DC-Ad-p53 vaccine as previously described²⁹. Treatment with UA was started three days after the first immunization and was continued for two weeks. Control groups included mice treated with UA alone, vaccine alone, or untreated. Immunization of mice bearing established tumors resulted in only temporal delay of tumor growth. It resumed 7 days after finish of the treatment. UA alone only marginally delayed tumor growth. In contrast, combination of vaccination with UA resulted in a substantial delay in tumor growth (Fig. 6f).

Discussion

MDSC are produced in response to a variety of tumor-derived cytokines and represent a mix population of myeloid cells at different stages of differentiation^{7,10,30-32}. Besides cancer, an increased production of MDSC was also reported in a number of pathological conditions including traumatic stress, bacterial and parasitic infections³³⁻³⁵. Recent studies from several groups have implicated MDSC in tumor-associated T-cell tolerance^{4,5}. To understand the mechanism of this phenomenon we used an experimental model with an adoptive transfer of T cells and MDSC into naïve congenic recipient. Tumor-free recipients allowed us to avoid the various confounding effects of tumor. In both tested experimental systems MDSC induced a marked decrease in the binding of specific pMHC to CD8⁺ T cells. Although this effect was not previously described in cancer, it is known that the changes in TCR binding avidity can play an important role in regulating antigen sensitivity³⁶⁻³⁸. More discussion is provided in supplement.

Our experiments demonstrated a critical role of ROS in MDSC-mediated T-cell tolerance. ROS can modify proteins directly or in combination with NO contributing to generation of peroxynitrite. In this study, the use of peroxynitrite scavenger completely eliminated MDSC-induced T-cell tolerance. Nitration of tyrosine is being long recognized as a marker of peroxynitrite activity. Peroxynitrite-dependent tyrosine nitration is likely to occur through the initial reaction of peroxynitrite with carbon dioxide or metal centers leading to secondary nitrating species as nitrogen dioxide radicals³⁹. In addition, peroxynitrite can react directly with cysteine, methionine and tryptophan³⁹. It is likely that tyrosine nitration represents only part of overall peroxynitrite activity in this experimental system.

Molecular modeling revealed a number of tyrosine residues in TCR and CD8 molecules that could be susceptible to nitration and structural analysis showed that nitration of these residues would result in the decreased flexibility and increased rigidity of TCR domains that might significantly alter the epitope-specific interactions between TCR and pMHC. Substantially higher levels of NT on the surface of antigen-specific CD8⁺ T cells from mice treated with MDSC confirm the antigenic specificity of the tolerance induced by contacts with MDSC.

These results suggest a new mechanism of CD8⁺ T cell tolerance in cancer and possibly in other pathological conditions associated with accumulation of MDSC. MDSC accumulated in tumor-bearing hosts contain high levels of ROS and peroxynitrite. Since these substances are

short-lived and highly reactogenic, they are active only at very short distance. Interface of MDSC and CD8⁺T cells interacting during antigen-TCR recognition provides such an environment. The amount of peroxynitrite produced by MDSC is sufficient to nitrate tyrosine exposed on the surface of contacting cells. Modified tyrosine on TCR and CD8 alter the conformational flexibility of TCR chains that lead to loss of the response to specific antigen. We suggest that similar scenario of tumor-induced peripheral immunological tolerance may potentially operate using other post-translational modifications of proteins from the TCR-pMHC complex. This mechanism may explain the well-established fact that tumor-bearing hosts don't have a profound systemic immune deficiency and T cells retain their ability to respond to other stimuli including viruses, lectins, IL-2, etc. This study provides additional support to the attempt of preventing the nitrotyrosine formation in cancer immunotherapy⁴⁰. Block of peroxynitrite generation or use of scavengers could represent an attractive opportunity to decrease or even eliminate MDSC-induced T-cell tolerance and enhance the effect of cancer immunotherapy. Other potential molecular targets could be discovered if other tumor-induced post-translational modifications of proteins involved in T cell-APC interactions would be explored.

Materials and Methods

Mice and reagents

All mouse experiments were approved by University of South Florida Institutional Animal Care and Use Committee. Female C57BL/6 mice (6-8 weeks of age) were obtained from the National Cancer Institute. OT-1 TCR-transgenic mice (*C57Bl/6-Tg(TCR α TCR β)1100mjb*), *gp91^{pho}-/-* (B6.129S6-*Cybb^{tm1Din}*), *iNOS^{-/-}* (C57BL6-Nos2^{tm1Lau}), and CD45.1⁺ congenic mice (B6.SJL-PtcaPep3b/BoyJ) were purchased from Jackson Laboratories. 2C TCR transgenic mice were described earlier⁴¹. To establish tumors, C57BL/6 mice were injected s.c. with 5×10^5 EL-4 or EG-7 cells.

OVA-derived (H-2K^b, SIINFEKL), 2C-specific (H-2K^b, SIYRYYYGL (SIY and H-2L^d QLSPFPFDL (QL9)), and control H-2K^b RAHYNIVTF peptides were obtained from QCB. IFA and UA were purchased from Sigma Chemical Co. All antibodies used for flow cytometry were obtained from BD Pharmingen except anti-NT (Upstate USA Inc.)

Cell isolation and generation

Gr-1⁺ cells were isolated from spleens of tumor-bearing mice using magnetic beads and MiniMACS columns (Miltenyi Biotec GmbH) and biotinylated anti-Gr-1 antibody. More than 98% of Gr-1⁺ cells were also CD11b⁺ (Fig. S1). T lymphocytes were isolated from spleens using T-cell enrichment columns (R&D Systems). DCs were generated from murine bone marrow using GM-CSF (Invitrogen) and IL-4 (R&D Systems) as described before⁴². DCs were activated on day 6 of culture by overnight incubation with LPS (1 μ g/ml). On day 7 cells were collected and DCs were enriched by centrifugation over Nycoprep A gradient (Accurate Chemicals). To pulse DCs with peptide, cells were washed in PBS and incubated with either specific or control peptides (10 μ g/ml) at 37° C for 2 h.

Adoptive cell transfer and immunization

$4-5 \times 10^6$ of purified T cells from OT-1 or 2C TCR transgenic mice were injected intravenously (i.v.) into naive C57BL/6 recipient mice. Two-three days later these mice were injected i.v. with $4-5 \times 10^6$ MDSC and within an hour immunized subcutaneously with 100 μ g of specific peptides in IFA. Ten days later cells from LN were re-stimulated with specific or control peptides and analyzed (Fig. S1).

ELISPOT

The number of IFN- γ producing cells in response to stimulation to the specific or control peptides (10 μ g/ml) was evaluated in ELISPOT assay performed as described earlier⁴³. Each well contained 2×10^5 LN cells. The number of spots were counted in triplicates and calculated using an automatic ELISPOT counter (Cellular Technology, Ltd).

Antigen Binding assay

Fluorescently labeled H2-K^b—Ig dimers were prepared as described previously³⁶ and dimers binding to T cells was measured by flow cytometry using a FACScalibur (Becton Dickinson). Specific binding of the dimer was calculated by subtracting nonspecific binding (using K^b-Ig loaded with irrelevant peptide) from the total binding.

Immunoprecipitation

T cells were collected, washed in PBS and lysed. Anti-CD8, or anti-TCR β antibodies were added to lysates (500 μ g of protein per sample) and incubated for 2 h at 4°C followed by the addition of protein A Sepharose beads (eBioscience). After 1 h incubation protein/antibody/beads mix was washed, re-suspended in Laemmli SDS sample buffer and denatured at 95°C for 5 min. Samples were resolved in 10 % SDS-PAGE followed by transfer to PVDF membrane and probing with anti-NT, CD8, or TCR β antibodies.

Molecular modeling of TCR/H-2K^b/peptide complex

The Biopolymer module of the SYBYL 7-1 software package (TRIPOS, Inc.) was used to analyze structural effects of the TCR nitration on the interactions within the TCR-MHC/peptide complex. The crystal structure of the TCR/H-2K^b/SIYRYYYGL and TCR/H-2K^b/EQYKFYSV complexes (PDB codes:1G6R, 2CKB and 1MWA) were used as templates for modeling and analysis of intermolecular interactions for both native and nitrated TCR/MHC/peptide complexes. After adding all hydrogens to crystal structures, the molecular structures were energy-minimized using the MMFF94s force field implemented in SYBYL. Energy minimizations were performed by 300 cycles of conjugate gradient minimization, and potential hydrogen bonds were visualized and analyzed with Biopolymer.

Confocal microscopy

Splenocytes from OT-1 mice were cultured with specific peptide in the presence of MDSC (at 3:1 ratio) on a poly-d-lysine coated glass bottom culture dish (MatTek Corp.). The cells were labeled with anti-Gr-1-PE, anti-CD8-Alexa 647, anti-Nitrotyrosine-Alexa 488, or isotype IgG Alexa 488. Cells were viewed with a DMI6000 inverted Leica TCS AOBS SP5 tandem scanning confocal microscope with a 40x/1.30NA oil immersion objective. Tunable 488 Argon and 546 and 633 laser lines were applied to excite the samples using AOBS line switching to minimize crosstalk between fluorochromes. Images and Z-stacks were produced with three cooled photomultiplier detectors and the LAS AF version 1.5.1.889 software suite.

Supplementary Material

Refer to Web version on PubMed Central for supplementary material.

Acknowledgments

We thank Dr. S. Kusmartsev for his assistance at the beginning of this project and Mrs J. DeComarmond for technical assistance with preparation of manuscript.

This work was supported by NIH grant RO1CA 84488 to DIG. This work has been supported in part by the Analytic Microscopy and Flow Cytometry Core Facility at the H. Lee Moffitt Cancer Center.

This paper complies with Nature Publishing policy concerning image integrity.

S.N. performed most of the experiments and wrote the manuscript, K.G. performed some of binding experiments, V.P. contributed to overall research design and molecular modeling analysis, L.K. performed molecular modeling analysis, S.S. performed molecular modeling analysis, L.K. performed immunohistology in human tissues, D.H. performed immunohistology in mouse tissues; J.S. contributed to overall research design and analysis, D.I.G. designed the experiments, analyzed the data, wrote the manuscript, and supervised the project.

Abbreviation

MDSC, myeloid derived suppressor cells; DC, dendritic cells; pMHC, peptide-MHC; ROS, reactive oxygen species; NO, nitric oxide; UA, uric acid; NT, nitrotyrosine.

References

1. Pardoll D. Does the immune system see tumors as foreign or self? *Annu. Rev. Immunol* 2003;21:807–839. [PubMed: 12615893]
2. Sotomayor EM, et al. Conversion of tumor-specific CD4+ T-cell tolerance to T-cell priming through in vivo ligation of CD40. *Nat. Med* 1999;5:780–787. [PubMed: 10395323]
3. Cuenca A, et al. Extra-lymphatic solid tumor growth is not immunologically ignored and results in early induction of antigen-specific T-cell anergy: dominant role of cross-tolerance to tumor antigens. *Cancer. Res* 2003;63:9007–9015. [PubMed: 14695219]
4. Kusmartsev S, Nagaraj S, Gabrilovich DI. Tumor-associated CD8+ T cell tolerance induced by bone marrow-derived immature myeloid cells. *J. Immunol* 2005;175:4583–4592. [PubMed: 16177103]
5. Huang B, et al. Gr-1+CD115+ immature myeloid suppressor cells mediate the development of tumor-induced T regulatory cells and T-cell anergy in tumor-bearing host. *Cancer. Res* 2006;66:1123–1131. [PubMed: 16424049]
6. Serafini P, Borrello I, Bronte V. Myeloid suppressor cells in cancer: recruitment, phenotype, properties, and mechanisms of immune suppression. *Semin. Cancer. Biol* 2006;16:53–65. [PubMed: 16168663]
7. Gabrilovich D. The mechanisms and functional significance of tumour-induced dendritic-cell defects. *Nat. Rev. Immunol* 2004;4:941–952. [PubMed: 15573129]
8. Kusmartsev S, Gabrilovich DI. Role Of Immature Myeloid Cells in Mechanisms of Immune Evasion In Cancer. *Cancer. Immunol. Immunother* 2006;55:237–245. [PubMed: 16047143]
9. Sinha P, Clements VK, Miller S, Ostrand-Rosenberg S. Tumor immunity: a balancing act between T cell activation, macrophage activation and tumor-induced immune suppression. *Cancer. Immunol. Immunother* 2005;54:1137–1142. [PubMed: 15877228]
10. Almand B, et al. Increased production of immature myeloid cells in cancer patients. A mechanism of immunosuppression in cancer. *J. Immunol* 2001;166:678–689. [PubMed: 11123353]
11. Schmielau J, Finn OJ. Activated granulocytes and granulocyte-derived hydrogen peroxide are the underlying mechanism of suppression of T-cell function in advanced cancer patients. *Cancer. Res* 2001;61:4756–4760. [PubMed: 11406548]
12. Zea AH, et al. Arginase-producing myeloid suppressor cells in renal cell carcinoma patients: a mechanism of tumor evasion. *Cancer. Res* 2005;65:3044–3048. [PubMed: 15833831]
13. Appleman LJ, Tzachanis D, Grader-Beck T, van Puijenbroek AA, Boussiotis VA. Helper T cell anergy: from biochemistry to cancer pathophysiology and therapeutics. *J. Mol. Med* 2001;78:673–683. [PubMed: 11434720]
14. Steinman RM, Nussenzweig MC. Avoiding horror autotoxicus: the importance of dendritic cells in peripheral T cell tolerance. *Proc. Natl. Acad. Sci. USA* 2002;99:351–358. [PubMed: 11773639]
15. Kusmartsev S, Gabrilovich DI. Inhibition of myeloid cell differentiation in cancer: The role of reactive oxygen species. *J. Leukoc. Biol* 2003;74:186–196. [PubMed: 12885935]
16. Dutz JP, Tsomides TJ, Kageyama S, Rasmussen MH, Eisen HN. A cytotoxic T lymphocyte clone can recognize the same naturally occurring self peptide in association with a self and nonself class I MHC protein. *Mol. Immunol* 1994;31:967–975. [PubMed: 8084337]
17. Udaka K, Wiesmuller KH, Kienle S, Jung G, Walden P. Self-MHC-restricted peptides recognized by an alloreactive T lymphocyte clone. *J. Immunol* 1996;157:670–678. [PubMed: 8752916]

18. Quinn, MT. The neutrophils respiratory burst oxidase. In: Gabrilovich, DI., editor. *The neutrophils. New outlook for old cells.* Imperial College Press; London: 2005. p. 35-85.
19. Squadrito GL, Pryor WA. The formation of peroxynitrite in vivo from nitric oxide and superoxide. *Chem. Biol. Interact* 1995;96:203–206. [PubMed: 7728908]
20. Kusmartsev S, Nefedova Y, Yoder D, Gabrilovich DI. Antigen-specific inhibition of CD8+ T cell response by immature myeloid cells in cancer is mediated by reactive oxygen species. *J. Immunol* 2004;172:989–999. [PubMed: 14707072]
21. Regoli F, Winston GW. Quantification of total oxidant scavenging capacity of antioxidants for peroxynitrite, peroxy radicals, and hydroxyl radicals. *Toxicol. Appl. Pharmacol* 1999;156:96–105. [PubMed: 10198274]
22. Balavoine GG, Geletii YV. Peroxynitrite scavenging by different antioxidants. Part I: convenient assay. *Nitric Oxide* 1999;3:40–54. [PubMed: 10355895]
23. Smyth M, et al. Tumor necrosis factor-related apoptosis-inducing ligand (TRAIL) contributes to the interferon-gamma-dependent natural killer cell protection from tumor metastasis. *J. Exp. Med* 2000;193:661.
24. Kusmartsev S, Gabrilovich D. STAT1 signaling regulates tumor-associated macrophage-mediated T cell deletion. *J. Immunol* 2005;174:4880–4891. [PubMed: 15814715]
25. Zingarelli B, et al. Oxidation, tyrosine nitration and cytostasis induction in the absence of inducible nitric oxide synthase. *Int. J. Mol. Med* 1998;1:787–795. [PubMed: 9852297]
26. Haqqani AS, Kelly JF, Birnboim HC. Selective nitration of histone tyrosine residues in vivo in mutated tumors. *J. Biol. Chem* 2002;277:3614–3621. [PubMed: 11723112]
27. Quint P, Reutzel R, Mikulski R, McKenna R, Silverman DN. Crystal structure of nitrated human manganese superoxide dismutase: mechanism of inactivation. *Free Radic. Biol. Med* 2006;40:453–458. [PubMed: 16443160]
28. Wilkinson IB, MacCallum H, Cockcroft JR, Webb DJ. Inhibition of basal nitric oxide synthesis increases aortic augmentation index and pulse wave velocity in vivo. *Br. J. Clin. Pharmacol* 2002;53:189–192. [PubMed: 11851643]
29. Nikitina EY, et al. An effective immunization and cancer treatment with activated dendritic cells transduced with full-length wild-type p53. *Gene Therapy* 2002;9:345–352. [PubMed: 11938454]
30. Pandit R, Lathers D, Beal N, Garrity T, Young M. CD34+ immune suppressive cells in the peripheral blood of patients with head and neck cancer. *Ann. Otol. Rhinol. Laryngol* 2000;109:749–754. [PubMed: 10961808]
31. Bronte V, Serafini P, Appoloni E, Zanovello P. Tumor-induced immune dysfunctions caused by myeloid suppressor cells. *J. Immunoth* 2001;24:431–446.
32. Melani C, Chiodoni C, Forni G, Colombo MP. Myeloid cell expansion elicited by the progression of spontaneous mammary carcinomas in c-erbB-2 transgenic BALB/c mice suppresses immune reactivity. *Blood* 2003;102:2138–2145. [PubMed: 12750171]
33. Makarenkova VP, Bansal V, Matta BM, Perez LA, Ochoa JB. CD11b+/Gr-1+ myeloid suppressor cells cause T cell dysfunction after traumatic stress. *J. Immunol* 2006;176:2085–2094. [PubMed: 16455964]
34. Mencacci A, et al. CD80+Gr-1+ myeloid cells inhibit development of antifungal Th1 immunity in mice with candidiasis. *J. Immunol* 2002;169:3180–3190. [PubMed: 12218136]
35. Atochina O, Daly-Angel T, Piskorska D, Harn D. A shistosome expressed immunomodulatory glycoconjugate expand peritoneal Gr1+ macrophages that suppress naïve CD4+ T cell proliferation via an interferon-gamma and nitric oxide dependent mechanism. *J. Immunol* 2001;167:4293–4302. [PubMed: 11591752]
36. Fahmy TM, Bieler JG, Edidin M, Schneck JP. Increased TCR avidity after T cell activation: a mechanism for sensing low-density antigen. *Immunity* 2001;14:135–143. [PubMed: 11239446]
37. Maile R, et al. Peripheral “CD8 tuning” dynamically modulates the size and responsiveness of an antigen-specific T cell pool in vivo. *J. Immunol* 2005;174:619–627. [PubMed: 15634879]
38. Drake DR 3rd, Ream RM, Lawrence CW, Braciale TJ. Transient loss of MHC class I tetramer binding after CD8+ T cell activation reflects altered T cell effector function. *J. Immunol* 2005;175:1507–1515. [PubMed: 16034088]

39. Alvarez B, Radi R. Peroxynitrite reactivity with amino acids and proteins. *Amino Acids* 2003;25:295–311. [PubMed: 14661092]
40. De Santo C, et al. Nitroaspirin corrects immune dysfunction in tumor-bearing hosts and promotes tumor eradication by cancer vaccination. *Proc. Natl. Acad. Sci. U S A* 2005;102:4185–4190. [PubMed: 15753302]
41. Sha WC, et al. Selective expression of an antigen receptor on CD8-bearing T lymphocytes in transgenic mice. *Nature* 1988;335:271–274. [PubMed: 3261843]
42. Kusmartsev S, et al. All-trans-retinoic acid eliminates immature myeloid cells from tumor-bearing mice and improves the effect of vaccination. *Cancer. Res* 2003;63:4441–4449. [PubMed: 12907617]
43. Gabilovich DI, Velders M, Sotomayor E, Kast WM. Mechanism of immune dysfunction in cancer mediated by immature Gr-1+ myeloid cells. *J. Immunol* 2001;166:5398–5406. [PubMed: 11313376]

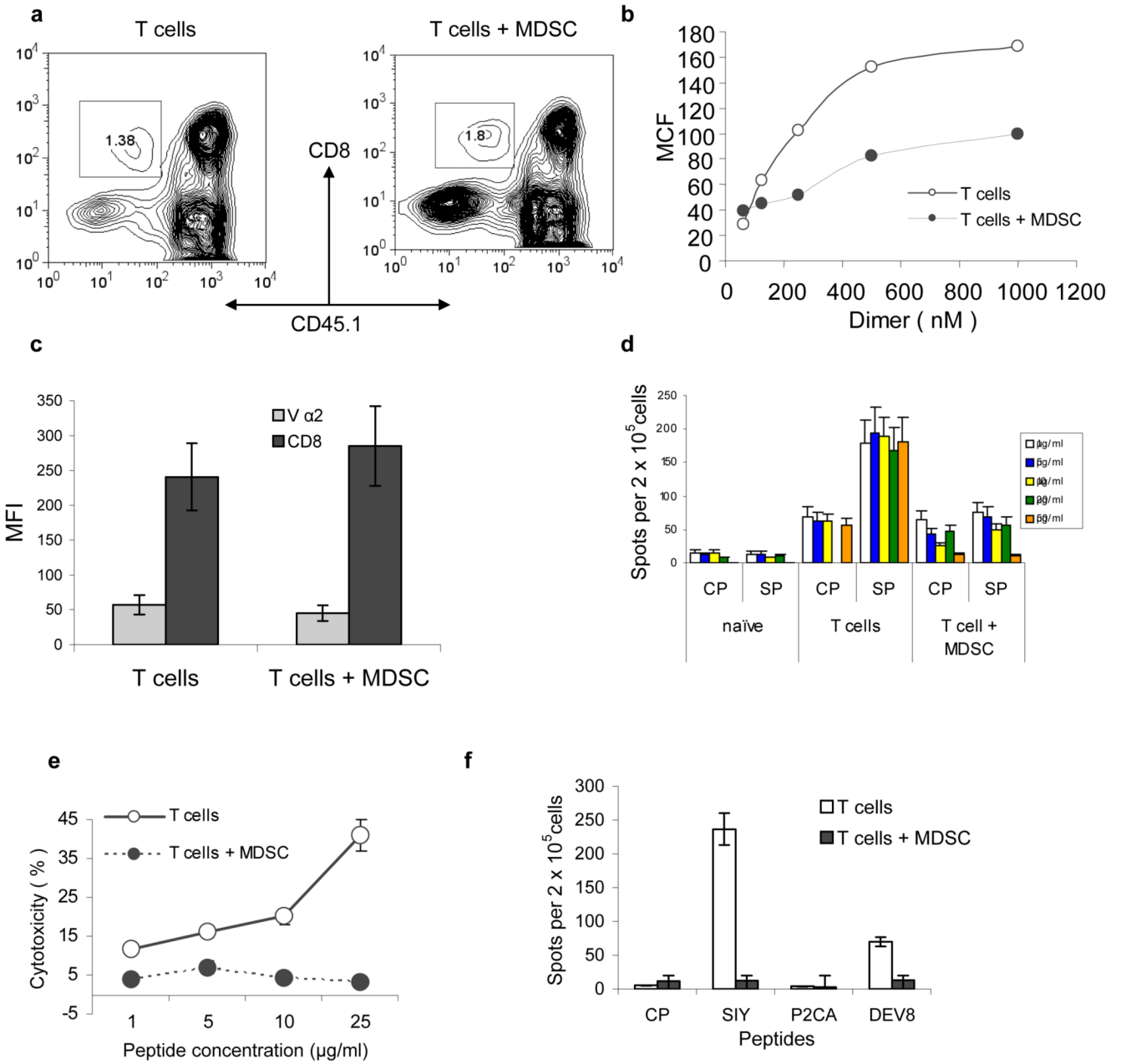


Figure 1. MSDC disrupt binding of pMHC to CD8⁺ T cells

(a) OT-1 T cells (CD45.1⁻) were transferred to naïve congenic (CD45.1⁺) recipients. Adoptive transfer of MDSC and immunization were performed as described in Methods. LN cells were collected 10 days later and were gated for donor's CD45.1⁻ CD8⁺ T cells. T cells alone – no MDSC transfer was performed. Typical example of 8 performed experiments is shown.

(b) CD45.1⁻ CD8⁺ OT-1 T cells were incubated with various amount of PE-conjugated MHC-Ig (1.20×10^{-6} to 6.25×10^{-8} M). Binding was determined by flow cytometry. MCF-mean channel fluorescence. The level of fluorescence of non-specific dimer (SIYRYYYGL-K^b-Ig) was subtracted from the values of fluorescence obtained with specific dimer (SIINFEKL- K^b-Ig). T – T cells from control mice T+MDSC- T cells from mice which received OT-1-T cells + MDSC. Three experiments with similar results were performed.

(c) The expression of CD8 and $V\alpha_2$ TCR from OT-1 mice was evaluated in antigen specific CD45.1⁻ CD8⁺ T cells from control and tolerized mice. The mean fluorescence \pm st. dev. from three different experiments are shown.

(d) Adoptive transfer of OT-1 cells, MDSC and immunization were performed as described above. Ten days later LN cells were restimulated in triplicates for 48 h with specific or control peptides at indicated concentrations. IFN- γ producing cells was scored in ELISPOT assay and calculated per 2×10^5 LN cells. Three experiments with the same results were performed. CP – re-stimulation with control peptide, SP- re-stimulation with specific peptide (SIINFEKL). Naïve – no adoptive transfer of OT-1 T cells was performed; T-cells – adoptive transfer of OT-1 T cells but no MDSC; T cells + MDSC – adoptive transfer of both OT-1 T cells and MDSC.

(e) Experimental design was as described above. Additional immunization was performed on day 8. Splenocytes were isolated on day 10 and tested in a standard 6 h ^{51}Cr -release CTL assay against the target EL-4 cells loaded with specific or control peptides at indicated concentrations. Cells were incubated in duplicates at 25:1 effector : target ratio. The levels of non-specific cytotoxicity (EL-4 target cells loaded with control peptide) were subtracted. Background cytotoxicity was less than 10%. Two experiments with similar results were performed.

(f) 2C T cells were transferred to naïve recipients followed by transfer of MDSC and immunization as described above and in Fig. S1. The following peptides were used for immunization: SIYRYYGL (**SIY**), LSPFPFDL (**P2CA**), and EQYKFYSV (**DEV8**). CP – control peptide (SIINFEKL). LN cells were collected 10 days later and were re-stimulated with corresponding peptides in an IFN- γ ELISPOT assay. Each group included three mice.

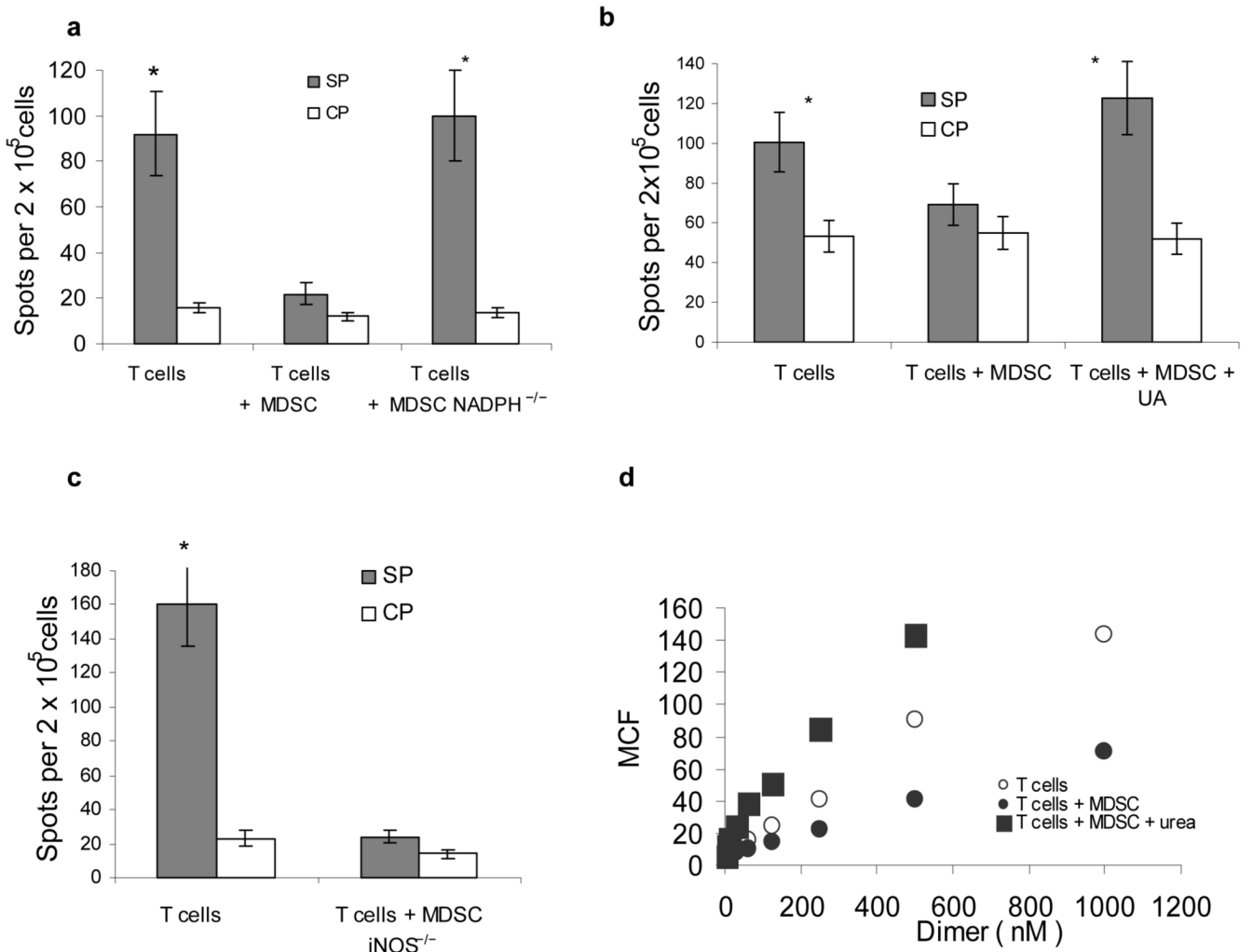


Figure 2. Mechanism of MDSC induced T-cell tolerance

Experimental design with adoptive transfer and immunization was as described in Fig 1.

(a–c) IFN- γ ELISPOT assay of LN cells re-stimulated with control (CP) or specific (SP) peptides was performed. Results presented as Average \pm SD per 2×10^5 LN cells. * - significant differences ($p < 0.05$) between CP and SP groups. (a) MDSC from EL-4 tumor-bearing NADPH^{-/-} (gp91^{phox}^{-/-}) or wild-type mice were used for adoptive transfer. Mean \pm st. dev. from three performed experiments are shown (b) Mice were treated with UA in suspension (20 mg in 100 μ l) on days -1, 0, 1, and 2 after MDSC transfer. (c) MDSC from EL-4 tumor-bearing iNOS^{-/-} mice were used for adoptive transfer. Two experiments with the same results were performed.

(d) LN cells from OT-1 mice were cultured with 10 μ g/ml SIINFEKL and MDSC (at 3:1 ratio) for 48 h in the presence of 1 mg/ml urea. After that time the binding of control and specific pMHC to CD8⁺ T cells was evaluated using flow cytometry as described in Fig. 1. T – T cells incubated without MDSC; T+MDSC- T cells incubated with MDSC; T + MDSC+Urea – T cells incubated with MDSC in the presence of urea.

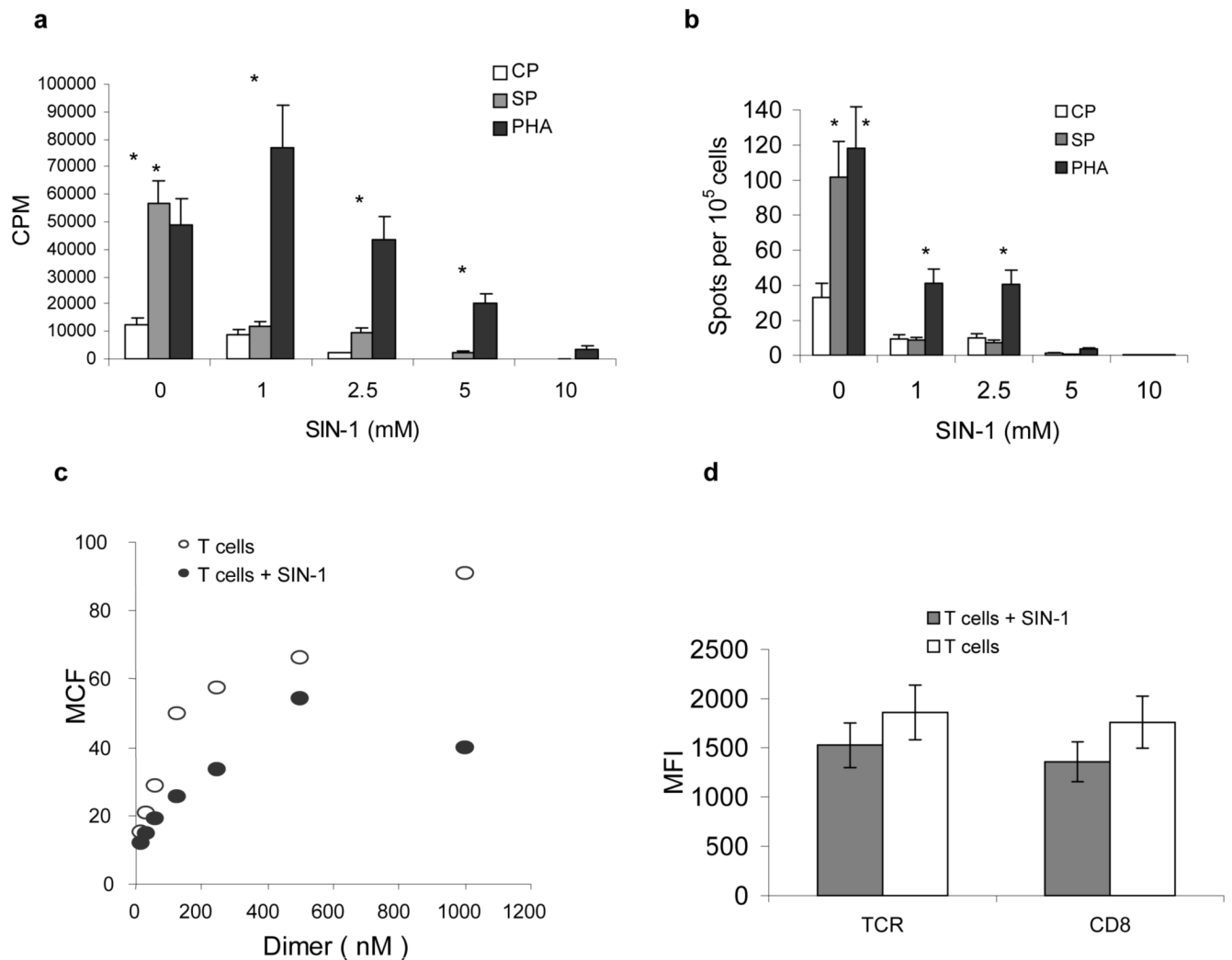


Figure 3. Effect of peroxynitrite donor on specific CD8⁺ T-cell activity

(a) OT-1 T cells were pretreated with SIN-1 (0 to 10 mM) for 30 min and then 5×10^4 T cells were cultured for 4 days with DCs at a 10:1 ratio. CP – DCs were loaded with 10 μ g/ml control (RAHYNIVTF) peptide, SP – DCs were loaded with 10 μ g/ml specific (SIINFEKL) peptide. PHA – OT-1 T cells and DCs were cultured for 3 days in the presence of 1 μ g/ml PHA. ³[H]-thymidine (1 μ Ci/well) was added 18 h prior to cell harvest and radioactivity was measured in triplicates in liquid scintillation counter. Results presented as Mean \pm SD.

(b) OT-1 T cells were cultured for 48 h with DCs, peptide and PHA as described in Fig. 3a. The number of IFN- γ producing cells was evaluated in quadruplicates in ELISPOT assay. Results presented as Mean \pm SD.

(c) OT-1 T cells were pretreated with 1 mM SIN-1 for 30 min. The binding of control and specific pMHC dimers to CD8⁺ T cells was evaluated using flow cytometry as described in Fig. 1. T – T cells stimulated with specific peptide-loaded DCs; T+Sin-1 – T cells pre-treated with SIN-1.

(d) Cells were treated as described in Fig. 3c and then labeled with anti-CD8 or anti-TCR $\alpha\beta$ antibodies. The levels of expression (mean fluorescence intensity, MFI) within the population of CD8⁺ T cells were evaluated by flow cytometry. The results of three experiments are shown.

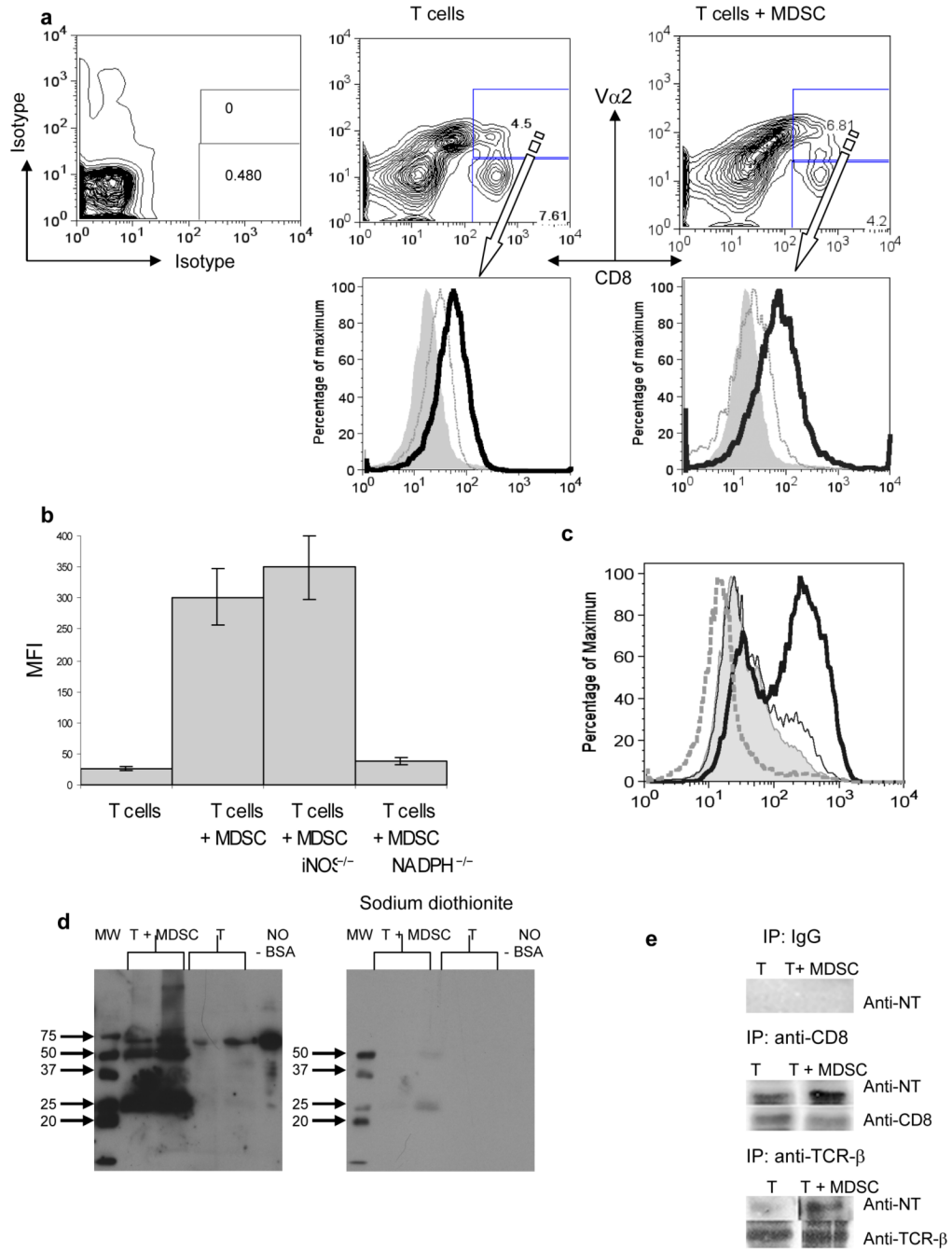


Figure 4. Role of MDSC in the nitration of tyrosine in a CD8⁺ T cell

(a) Adoptive transfer and immunization was performed as described in Figs 1 and S1. Eight days later LNs were isolated and labeled with anti-CD8, anti-V α ₂, and anti-NT antibodies. The level of NT expression was evaluated within population of donors (CD8⁺V α ₂⁺) (bold line) and recipient (CD8⁺V α ₂⁻) (thin line). Shaded areas show staining with isotype control IgG.

(b) Splenocytes from OT-1 mice were cultured with control or specific peptides for 72 h in the presence of MDSC (at 3:1 ratio) from wild-type, *NADPH*^{-/-} (*gp91*^{phox}^{-/-}) and *iNOS*^{-/-} EL-4 tumor-bearing mice. After that time cells were collected and the levels of NT in CD8⁺ T cells were evaluated by flow cytometry. Mean \pm SD of MFI from three experiments are shown. Not shown MFI for samples with control peptides, which were below 30 in all experiments.

(c) The level of NT in CD8⁺ OT-1 T cells. Cells were treated as described in Fig. 4b. Shaded area – splenocytes alone, bold line splenocytes + MDSC; dashed line 1 mM SOD was added; thin line – 1 mM L-NMMA was added. CD8⁺ cells were gated and NT expression was measured within this cell population. Not shown MFI for samples with control peptides, which were below 30 in all experiments.

(d) Splenocytes from OT-1 mice were cultured for 48 h with specific peptide in the presence of MDSC (at 3:1 ratio). Whole cell lysates were prepared and were subjected to 10%SDS-PAGE electrophoresis and probed with anti-NT antibody. Nitrated BSA was used as a positive control for NT staining. Bands were visualized using ECL. Chemical reduction of nitrotyrosine was done using sodium dithionite. The membrane was washed and probed with anti-NT antibody. Each experiment was performed in duplicates (shown).

(e) Splenocytes cells from OT-1 mice were treated as described above. Whole cell lysates were prepared and CD8 and TCR β were immunoprecipitated using specific antibodies as described in Methods. Rabbit IgG was used in control experiments. The proteins were subjected to 10% SDS-PAGE electrophoresis and probed with anti-NT antibody. To verify loading, the same blots were stripped and re-probed with anti-CD8 or anti-TCR β antibodies.

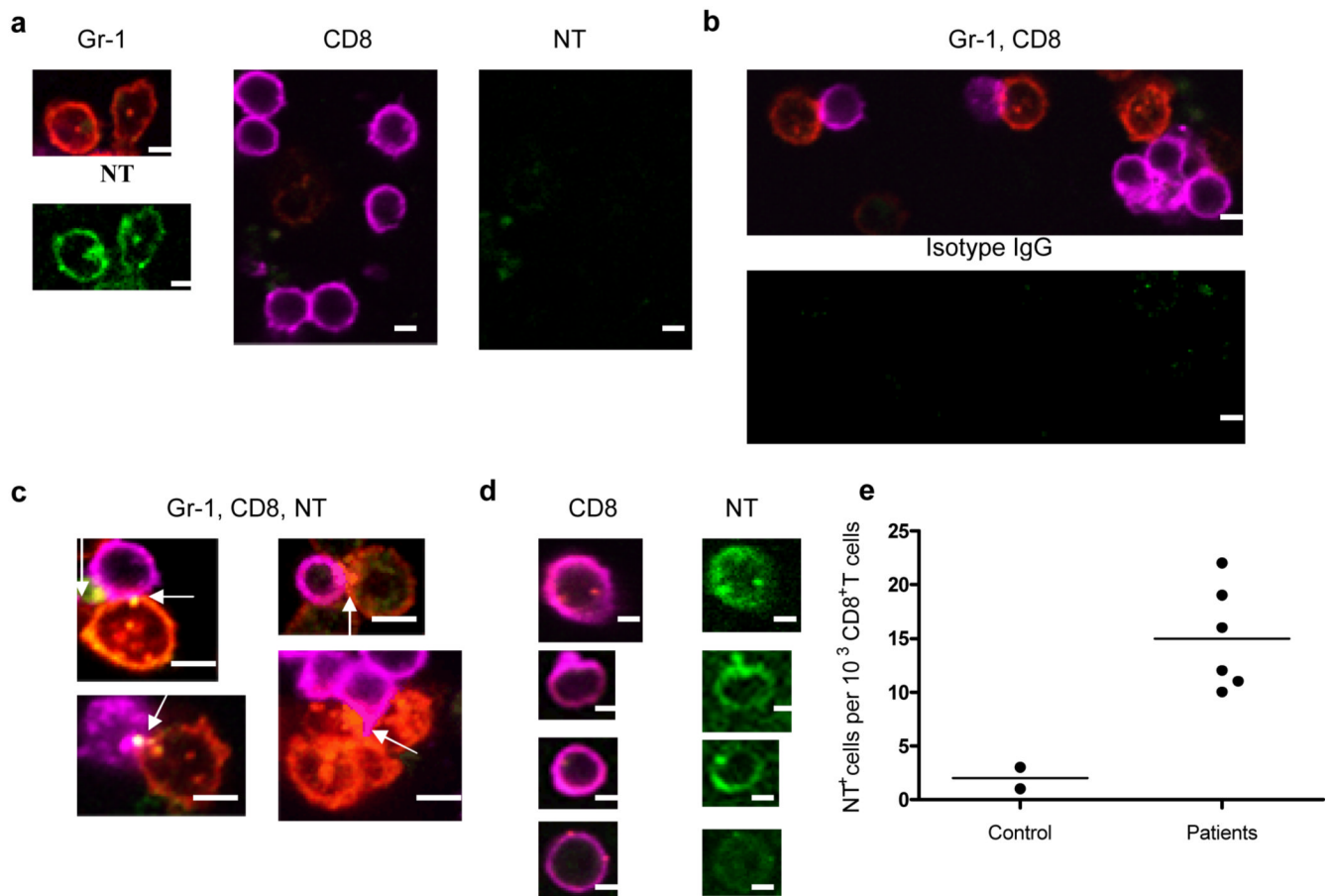


Figure 5. Interaction between MDSC and CD8⁺ T cells.

(a–d) Splenocytes from OT-1 mice were cultured with specific peptide and MDSC (at 3:1 ratio). The cells were labeled with anti-Gr-1-PE (red), anti-CD8-Alexa 647 (magenta), anti-NT-Alexa 488 (green), or isotype-Alexa 488 (green) at different time points and visualized under a confocal microscopy. Scale bar = 10 μ m. (a) MDSC and CD8 T cells separate; (b–c) 5 h co-culture. Arrows denote positive staining for NT localized at contacts between MDSC and CD8⁺ T cells. (d) 48 h culture.

(e) LN from individuals with breast and head and neck cancers were collected during tumor resection as part of routine pathological examination. LNs without presence of tumor were further evaluated (see Fig. S5). The number of NT positive cells per 10³ CD8⁺ T cells are shown.

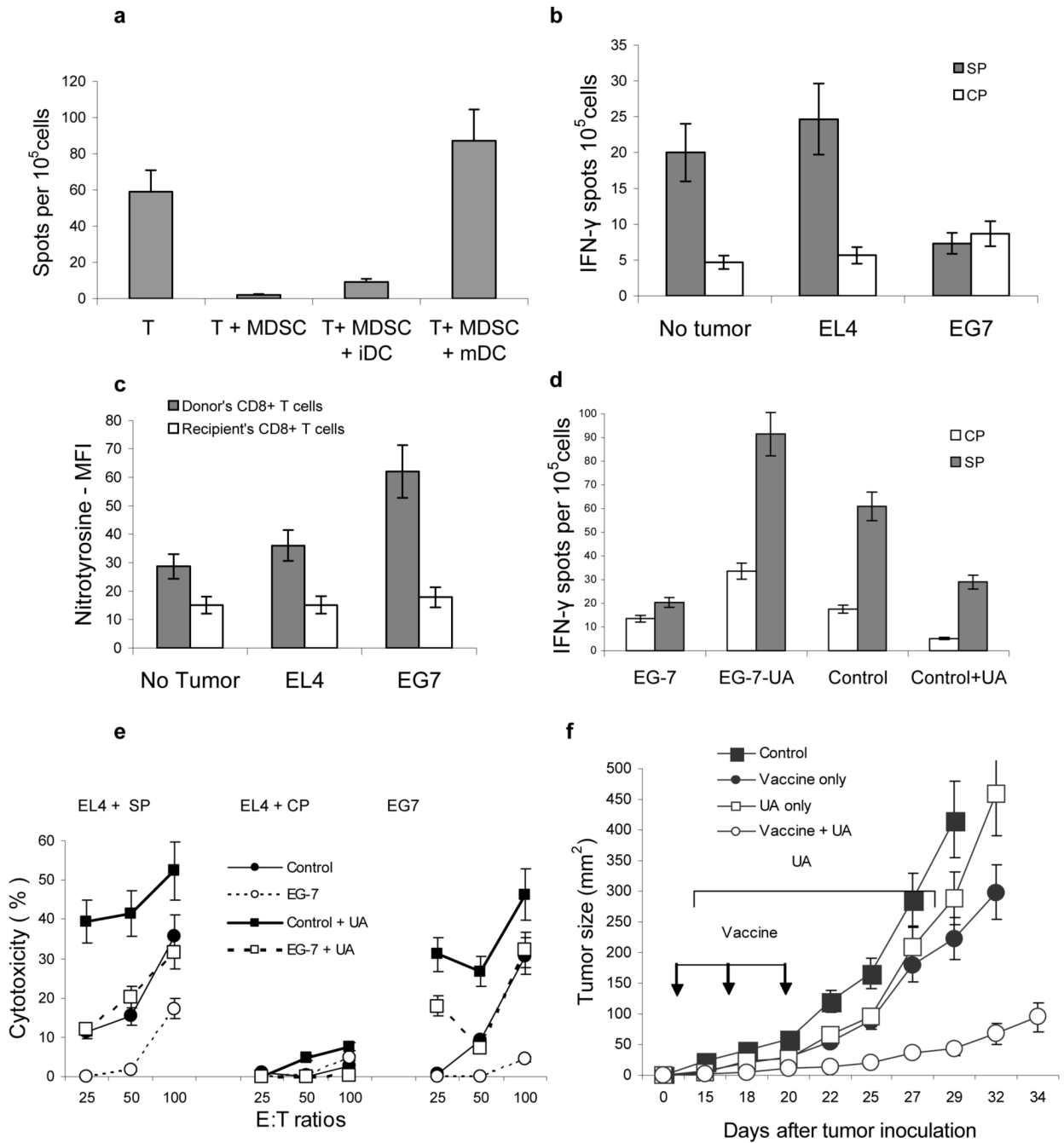


Figure 6. MDSC induced CD8⁺ T-cell tolerance in tumor-bearing mice

(a) Mice were treated as described in Fig. S1. Ten days after immunization LN cells were re-stimulated in triplicates with control or specific peptide or with bone marrow derived immature (iDC) or LPS activated matured (mDC) DCs. DCs were added at 1:10 ratio. The number of IFN- γ producing cells was measured in ELISPOT assay. Mean \pm st. dev. from two experiments are shown. The values of stimulation with control peptide were subtracted from the values of stimulation with specific peptide.

(b-e) C57BL/6 mice were inoculated subcutaneously with 5×10^5 of EL-4 or EG-7 tumor cells. Seven days after inoculation each mouse had been injected intravenously with 5×10^6 OT-1 T-cells. Seven days later mice were sacrificed and LN cells used in further experiments. (b) LN

cells were stimulated with specific (SP) (SIINFEKL) or control (CP) (RAHYNIVTF) peptides and analyzed in IFN- γ ELISPOT assay. The number of spots were calculated per 10^5 LN cells. Each group included 3 mice. The differences between SP and CP were statistically significant ($p < 0.05$) from control and EL-4 tumor-bearing mice. (c) Splenocytes were labeled with anti-CD8, anti-V α_2 , and anti-nitrotyrosine antibodies. The level of NT expression was evaluated within the populations of donors (CD8 $^+$ V α_2 $^+$) and recipient (CD8 $^+$ V α_2 $^-$) cells. MFI-mean fluorescence intensity. Results of the two performed experiments are shown. The differences between NT levels in donor's cells from EG-7 mice and EL-4 or control mice were statistically significant. (d) EG-7 tumor-bearing mice were treated with daily i.p. injections of UA (20 mg/100 μ l PBS) starting from the day of T-cell transfer. LN cells were collected 7 days later and analyzed in IFN- γ ELISPOT assay as described in Fig. 6b. (e) Splenocytes from EG-7 tumor-bearing mice described above were stimulated *ex vivo* for 7 days with SIINFEKL peptide 10 μ g/ml, in the presence of IL-15 (10 ng/ml) and IL-21 (10 ng/ml) and used as effectors in a standard 6-h 51 Cr-release CTL assay. Target cells were EL-4 cells pulsed with 10 μ g/ml of either specific (SIINFEKL) or control (RAHYNIVTF) peptides. In addition, EG7 cells were also used as targets. Different effector:target cell ratios were used. Each experiment was performed in duplicates and included three mice per group. Mean \pm st. dev. are shown. (f) MC38 tumor was established in C57BL/6 mice by subcutaneous injection of 2×10^5 tumor cells. On day 10 after tumor inoculation when tumors became palpable mice were split into four groups with equal tumor size. Each group included 5-6 mice. Mice in treatment group (vaccine + UA) were injected s.c with 5×10^5 DCs infected recombinant adenovirus containing mouse wild-type p53 gene as previously described²⁹. Immunizations were repeated twice with 5-6 day interval. Treatment with UA (20 mg/100 μ l PBS) was started three days after the first immunization and was continued for two weeks. Control groups included mice treated with UA alone (UA only), vaccine alone (vaccine only), or untreated (control). Tumor size was measured using calipers and presented as the result of multiplication of two longest dimensions. Mean \pm st. dev. are shown.